3-D pore geometry as a function of rock weathering: a CT-analysis

Ranjith P. Udawatta[A], Clark J. Gantzer[B], Stephen H. Anderson[B], Ann M. Rossi[C], Robert C. Graham[C] and Richard A. Ketcham[D]

[A]Center for Agroforestry and Department of Soil, Environmental and Atmospheric Sciences, School of Natural Resources, University of Missouri, MO 65211, USA, Email UdawattaR@missouri.edu
[B]Department of Soil, Environmental and Atmospheric Sciences, University of Missouri, MO 65211, USA.
[C]Department of Environmental Sciences, University of California, Riverside, CA 92521-0424, USA.
[D]Jackson School of Geosciences, University of Texas, Austin, TX 78712-1100, USA.

Abstract
An evaluation of geometrical pore parameters as influenced by rock weathering is helpful in understanding the development of soil. The objective of this study was to investigate three-dimensional (3-D) geometrical pore characteristics in rocks as affected by the degree of weathering. Rock fragments (clasts) from several moraines, ranging in age from 15-ky to 160-ky, were scanned using high-resolution X-ray computed tomography (CT) at 39–42 µm resolution. From each sample a 480×480×580 data block were extracted for analysis with 3-Dimensional Medial Axis Rock (3DMA-Rock) computer software. As weathering increased, samples developed more pores, and these pores were more extensively connected to other pores. Highly weathered samples had pores with the highest coordination numbers and characteristic coordination number constants. These parameters were significantly different from the un-weathered or partially weathered samples. More weathering also resulted in longer path lengths (PLs) and larger path length constants. PLs were < 2 mm for the un-weathered samples while partial and more fully weathered samples had values ranging up to 6 mm. The average tortuosity values decreased from 2.34 to 1.30 with weathering. Results indicated that 3-dimensional analysis of pore geometry can be used to discriminate rock weathering as well as to better understand the spatial variations in pore parameters.

Key Words
Moraine, pore connectivity, pore coordination number, pore path length, pore tortuosity, thresholding

Introduction

Soil formation from rock weathering is an on-going process which can be evaluated over time (Buol *et al*., 2003). Until recent years, weathering was extensively and intensively studied by examining physical and chemical changes in materials. These properties include changes in bulk density, porosity, texture, shape, form, surface features and chemistry. Although geometrical pore features affect the above properties, pore features are seldom examined at a high level of detail. Additionally, traditional procedures of pore evaluation are time consuming and provided no information on internal changes in the pore structure in 3-D as well as spatial differentiations within the structure.

In contrast, higher-resolution imaging techniques at µm- or sub-µm-scale can provide information on spatial variation of pores and geometrical differences in pore structure during rock weathering. Tomographic image slices can be acquired with X-ray, γ-radiation, or nuclear magnetic resonance energy techniques. By assembling contiguous cross-sectional images into data volumes, the three-dimensional distribution and nature of porosity can be visualized using a process called volume rendering, and additional 3D analysis tools can be used to quantify porosity information and geometrical pore parameters for rock, soil, and porous materials.

Quantitative information of rock weathering is required to improve our understanding of water and contaminant movement through materials, and to develop model parameters associated with fluid and gas transport. For example, Udawatta *et al*. (2008a) and Udawatta and Anderson (2008) compared medical X-ray CT-measured (190- by 190- by 500-µm) pore characteristics of various soils as influenced by soil management. These studies elucidated that number of pores, number of macropores, porosity, macroporosity, circularity, and fractal dimension of macropores correlated well with measured saturated hydraulic conductivity. In another study with images acquired at 85-µm resolution, pore tortuosity, connectivity, and other geometrical parameters correlated with management (Udawatta *et al*., 2008b). Comparing differences in throat size, tortuosity, and path characteristics between micro aggregates at 3.2 to 5.4 µm resolution, Peth *et al*. (2008) differentiated conventional tilled and grass soils. Using rock samples, Lindquist *et al*. (2000) compared tortuosity, pore connectivity, pore-channel length, and throat and nodal parameters of

Fontainebleau sandstone ranging from 7.5% to 22% porosity. The 5.7-µm resolution images distinguished sandstone material based on coordination numbers of nodal pores, and channel, pore, and throat parameters. However, the literature lacks 3-D evaluation of geometrical pore structure at µm resolution on rock weathering.

According to Birkeland (1999), moraines are well suited for studying rock weathering chronosequences since soil forming factors such as parent material, topography, biota, and climate are approximately constant. Thus, transformations with time can be examined. Evaluation of geometrical pore parameters at µm resolution will improve our understanding of rock weathering and help predict water transport and storage during rock weathering. The objective of the study was to test the hypothesis that internal 3-D geometrical pore parameters change during rock weathering. Analysis compared pore connectivity, pore paths, and tortuosity on weathered clasts from moraines with 3DMA-Rock computer software.

Materials and Methods

The clasts analyzed in this study were collected from moraines in the eastern Sierra Nevada, California, USA. Cosmogenic ^{36}Cl surface exposure dating has estimated that these materials were deposited between 15 ka and 170 ka (Phillips *et al*. in press).

Eight clasts were scanned at the High Resolution X-Ray CT facility at the University of Texas, Austin, USA. The X-ray scanner settings were 210 kV, 0.128 mA, with the intensity control set on, and with the high power mode using no filter. Slice spacing was 42 µm, and data for 25 slices were acquired in each turntable rotation. The raw data were corrected for X-ray fluctuations and ring artifacts prior to image reconstruction. Data were reconstructed as 1024×1024 16-bit TIFF images with a field of view of 40 µm, resulting in a pixel spacing of 39 µm. Contiguous scans were stacked to render 3-D volumes. To reduce edge effects, all samples were trimmed to 580 images, and then 480 by 480 pixel volumes were used for image analysis.

The 3DMA-Rock software was used for 3-D quantification of pore characteristics (Lindquist and Venkatarangan 1999). A number of algorithms are implemented in the image analysis software to accomplish the six main steps: segmentation of image, extraction and modification of the medial axis of pore paths, throat construction using the medial axis, pore surface construction, assembly of pore throat network, and geometrical characterization of pore throat network. Analysis followed information outlined in Lindquist *et al*. (2005) and generated information for: number of branch clusters and associated number of paths; as well as corresponding probabilities for coordination numbers, path lengths, path tortuosity, pore volume, effective radii, throat area, and throat radii. Only pore connectivity, pore path lengths, and path tortuosity and probability densities associated with these three parameters are presented to differentiate pore characteristics as affected by the degree of rock weathering.

Results

The coordination number (CN) characterizes pore topology, the number of paths meeting at one node. Figure 1 shows that the 15 ky sample had no pores with higher coordination-numbers while the 160 ky sample had the largest number of pores with higher CNs. The probabilities associated with these pores were higher than the partially weathered samples. In support of these scanning results, Rossi and Graham (in press) used the same rock material and observed 0.06 to 0.01% porosity formation per 1000 yrs using the bulk density method. Although the scanning method underestimates porosity, which depends on scanner resolution and thresholding, the bulk density and scanning methods both depicted the same trend, i.e., porosity increased with age. Results show that as rocks weather, they develop pores with higher CNs, i.e., more connected pores. The exponential distribution between CN and probability density had r^2 values between 0.62 and 0.92. Although the characteristic coordination number constant (Co) increases with more connected pores, the youngest sample with only a few pores resulted in a higher Co as compared to the two intermediate samples. This could be due to isolation of a smaller number of connected pores rather than sparsely distributed pores in the partially weathered samples.

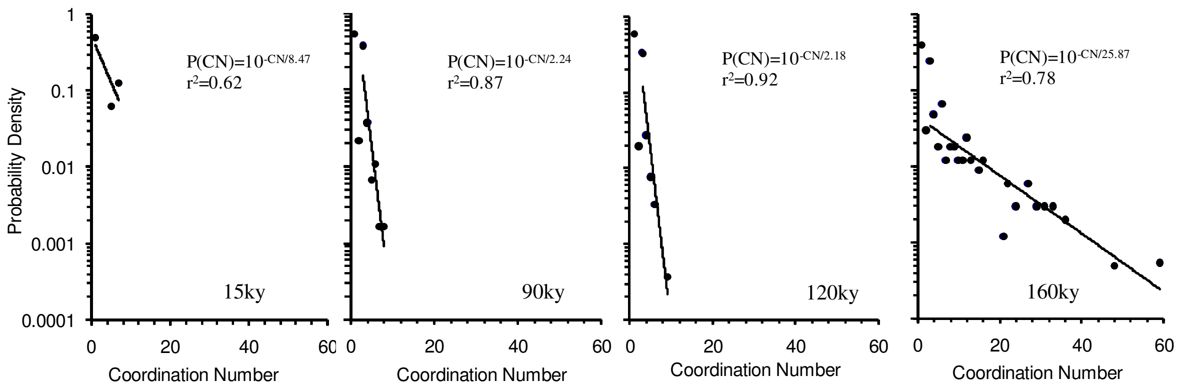

Figure 1. Probability density distribution vs. coordination numbers for 15-, 90-, 120-, and 160-ky age moraine samples from Sierra Nevada, California, USA.

Pore path lengths (PLs) ranged from 0.07 mm in the 15 ky sample to 6 mm in the other three samples (Figure 2). The 15 ky sample did not have PLs longer than 2 mm and they were significantly smaller than those of the other samples. Data also show that the 15 ky sample with smaller PLs had a narrower probability distribution range. Exponential relationships between the PLs and probability density resulted in the smallest path length constant (PLo) for the 15 ky sample (1.20) and the largest for the 160 ky sample (1.80). PLo values were in between for the moderately weathered samples (1.41 and 1.45). The exponential distribution resulted in r^2 values ranging from 0.62 and 0.93. Similar to these results, Udawatta *et al.* (2008b) observed increasing PLo for more porous soils as compared to less porous row crop soils in a CT study comparing agroforestry buffer and row crop soils. The results of this study also show that highly weathered samples possess pores with longer PLs and the probability for those pores is larger than the un-weathered or partially weathered samples.

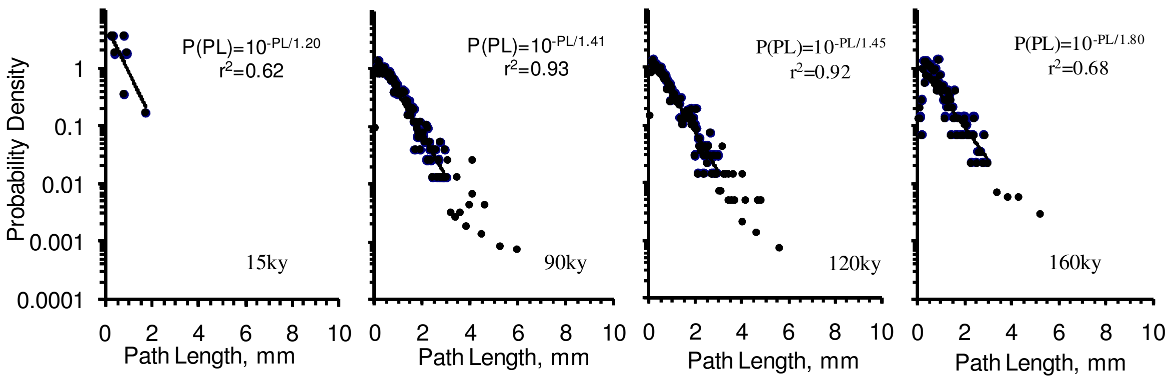

Figure 2. Probability density distribution vs. pore path length for 15-, 90-, 120-, and 160-ky age moraine samples from Sierra Nevada, California, USA.

Average path tortuosity decreased with rock weathering (Figure 3). Among the ten evaluated samples, the 15 ky sample had the highest average tortuosity (2.34) while the weathered samples had lower average values. The number of paths also varied among treatments with values being seven for the 15 ky sample to 34 for the 160 ky sample. The probability for pore path tortuosity decreased with increasing path tortuosity. However, the 15 ky sample had higher probabilities for higher tortuosities while the 160 ky sample had lower probabilities for higher tortuosities. The cumulative probability distributions of path tortuosity showed distinct differences among the treatments.

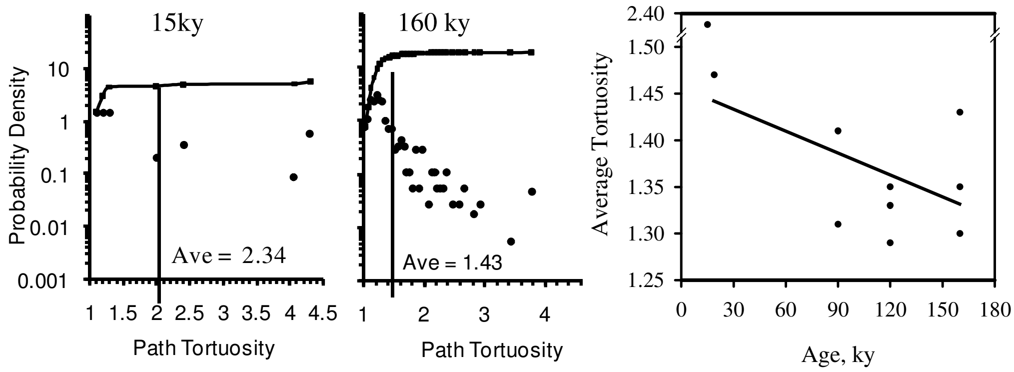

Figure 3. Probability density vs. path tortuosity (solid points) and cumulative probability density (solid line) for 15- and 160-ky samples. Average path tortuosity values for the ten examined samples with sample age.

Conclusions

Characteristic distributions of geometrical pore parameters were compared as influenced by rock weathering. Pore coordination numbers, path lengths, and path tortuosity changed during rock weathering. As pore structure develops and evolves, pores become connected with more pores, path lengths increase, and pore tortuosity decreases. Probabilities associated with these parameters increased as weathering proceeds. Results elucidate that analysis of high resolution images and 3-D visualization may assist in distinguishing geometrical pore parameters for better understanding of rock weathering. These results may help in predicting movement of liquids and gases within rocks as well as use of rock formations for storage of hazardous compounds. Future studies may be directed towards identifying a minimum set of parameters to discriminate gas and liquid transport through the material and understanding storage of hazardous materials for extended periods.

References

Birkeland PW (1999) 'Soil and Geomorphology'. 3rd Ed. (Oxford University Press: New York, NY, USA).

Buol SW, Southard RJ, Graham RC, McDaniel PA (2003) 'Soil Genesis and Classification'. (Iowa University Press: Ames, IA, USA).

Lindquist WB, Venkatarangan AB (1999) Investigating 3D geometry of porous media from high resolution images. *Physics and Chemistry of the Earth* (A) **25**, 593-599.

Lindquist WB, Venkatarangan AB, Dunsmuir JH, Wong TF (2000) Pore and throat size distributions measured from synchrotron X-ray tomographic images of Fontainebleau sandstones. *Journal of Geophysical Research* 105B, 21509-21528.

Lindquist WB, Lee SM, Oh W, Venkatarangan AB, Shin H, Prodanovic M (2005) 3DMA-Rock A Software Package for Automated Analysis of Rock Pore Structure in 3-D Computed Microtomography Images. [Online]. Available at http://www.ams.sunysb.edu/~lindquis/3dma/3dma_rock/3dma_rock.html (verified 18 September, 2009). Department of Applied Mathematics and Statistics, SUNY at Stony Brook, Stony Brook, NY, USA.

Peth S, Horn R, Beckmann F, Donath T, Fisher J, Smucker AJM (2008) Three-dimensional quantification of intra-aggregate porespace features using synchrotron-radiation-based microtomography. *Soil Science Society of America Journal* **72**, 897-907.

Phillips FM, Zreda M, Plummer MA, Elmore D, Clark DH (in press) Glacial geology and chronosequence of Bishop Creek and vicinity, eastern Sierra Nevada, California. *Geological Society of America Bulletin*.

Rossi AM, Graham RC (in press) Weathering and porosity formation in sub-soil granitic clasts, Bishop Creek Moraines, California. *Soil Science Society of America Journal* **74**, 172-185.

Udawatta RP, Anderson SH (2008) CT-measured pore characteristics of surface and subsurface soils influenced by agroforestry and grass buffers. *Geoderma* 145, 381-389.

Udawatta RP, Anderson SH, Gantzer CJ, Garrett HE (2008a) Influence of prairie restoration on CT-measured soil pore characteristics. *Journal of Environmental Quality* **37**, 219-228.

Udawatta RP, Gantzer CJ, Anderson SH, Garrett HE (2008b) Agroforestry and grass buffer effects on high resolution X-ray CT-measured pore characteristics. *Soil Science Society of America Journal* **72**, 295-304.